PNAS RESEARCH ARTICLE | ENVIRONMENTAL SCIENCES ECOLOGY

Entropy-based early detection of critical transitions in spatial vegetation fields

Giulio Tirabassi[a,1] and Cristina Masoller[a]

Edited by Alan Hastings, University of California, Davis, CA; received September 22, 2022; accepted November 8, 2022

In semiarid regions, vegetated ecosystems can display abrupt and unexpected changes, i.e., transitions to different states, due to drifting or time-varying parameters, with severe consequences for the ecosystem and the communities depending on it. Despite intensive research, the early identification of an approaching critical point from observations is still an open challenge. Many data analysis techniques have been proposed, but their performance depends on the system and on the characteristics of the observed data (the resolution, the level of noise, the existence of unobserved variables, etc.). Here, we propose an entropy-based approach to identify an upcoming transition in spatiotemporal data. We apply this approach to observational vegetation data and simulations from two models of vegetation dynamics to infer the arrival of an abrupt shift to an arid state. We show that the permutation entropy (PE) computed from the probabilities of two-dimensional ordinal patterns may provide an early warning indicator of an approaching tipping point, as it may display a maximum (or minimum) before decreasing (or increasing) as the transition approaches. Like other spatial early warning indicators, the spatial permutation entropy does not need a time series of the system dynamics, and it is suited for spatially extended systems evolving on long time scales, like vegetation plots. We quantify its performance and show that, depending on the system and data, the performance can be better, similar or worse than the spatial correlation. Hence, we propose the spatial PE as an additional indicator to try to anticipate regime shifts in vegetated ecosystems.

tipping-points | permutation-entropy | vegetation dynamics

Significance

Ecosystems can display abrupt regime shifts that oftentimes are irreversible. Anticipating these changes, such as desertification of semiarid areas, or forest-to-savanna transitions, is crucial for land management and the resilience of the human communities depending on these ecosystems. So far, many data-driven approaches have been proposed to infer indicators of approaching regime shifts. Here, we use observed and simulated data to study the performance of the spatial permutation entropy as an indicator of approaching vegetation shifts.

Ecological systems are known to display abrupt transitions between different states. Examples of dangerous transitions include population extinctions (1, 2), plankton blooms (3), algae blooms (4), and desertification (5–7), among others. In particular, due to their high ecological and social impact, tipping points in semiarid ecosystems, such as forest/savanna transitions and desertification, have gained much attention in the past years, and a lot of effort has been devoted to finding reliable early warning indicators for such abrupt shifts.

From a dynamical systems perspective, a transition to a different state is often modeled as a bifurcation that destroys a stable solution (e.g., a fixed point, a limit cycle, or an attractor) or changes its stability and may generate new solutions. Dynamical systems close to a bifurcation exhibit what is known as "critical slowing down" (CSD) (8): as the system approaches the tipping point, its dynamics become slower, and the relaxation time to equilibrium increases.

Several indicators have been designed to detect CSD, such as significant changes in variance or autocorrelation (9, 10), which found successful application in several real-world systems (11, 12). However, they may fail to predict transitions early enough to reverse them or mitigate their effects (13, 14). Additionally, CSD is often measured by employing time series analysis. Time series acquisition can be problematic for those systems where the characteristic timescale is particularly long, such as vegetation dynamics. Hence, there have been several attempts to link the CSD to spatial properties that can be easier to measure (15–18), for example, through satellite imaging or drone surveys. An example is the spatial correlation, which found application for detecting CSD in simulated vegetation plots close to an abrupt transition to desertification (15). Other examples are the spatial variance (15, 19), the spatial skewness (15), and variations in the two dimensional (2D) Fourier spectrum (17). Nevertheless, studies involving spatial indicators have mainly employed synthetic datasets, with only few exceptions (5, 20).

In this work, we use two observational vegetation datasets recorded in different geographical regions with different resolutions and simulations of two vegetation dynamics models to test a possible indicator of an approaching transition. We use the

Author affiliations: [a]Departament de Física, Universitat Politècnica de Catalunya, Terrassa 08222, Spain

Author contributions: G.T. and C.M. designed research; G.T. performed research; G.T. analyzed data; and G.T. and C.M. wrote the paper.

The authors declare no competing interest.

This article is a PNAS Direct Submission.

[1]To whom correspondence may be addressed. Email: giulio.tirabassi@upc.edu.

This article contains supporting information online at http://www.pnas.org/lookup/suppl/doi:10.1073/pnas.2215667120/-/DCSupplemental.

Published December 29, 2022.

permutation entropy (PE) (21) to characterize the statistical properties of the spatial fields composing our datasets and link them to the presence of an upcoming tipping point. Although PE is a well-known tool for time series characterization, used in fields as diverse as photonics, biomedicine, sports science, and climatology (22), it has not yet been tested for the analysis of variations of a spatial field when a regime transition is approaching. The PE computed from spatial ordinal patterns is a measure of the disorder of the spatial field, and we show that it may capture relevant changes as a transition approaches. We quantify the performance of the spatial PE in relation to the spatial correlation, that is a classical indicator, and find that, depending on the dataset analyzed, the PE indicator outperforms or underperforms the classical one.

Data

High-Resolution Vegetation Data. High-resolution vegetation data from ref. 23 correspond to ground-truth vegetation transects for the Serengeti–Mara ecosystem in northern Tanzania and southern Kenya. The transects have a resolution of 30 m × 30 m and have been binarized in ref. 20 assigning to each cell only two classes, woodland or grassland, and finally paired with mean annual rainfall data. The datasets are available through the original articles (20, 23).

In this work, we use transect 5 (Fig. 1) because it presents a sharp transition between the two regions when varying the rainfall level. It also has a good density of points along the upper branch, which is of particular interest for understanding the transition from forest to savanna states (20). The transect covers an area of 7.53 km × 122.46 km corresponding to 251 × 4,082 cells. Zooming on the transition region reveals a small hysteresis loop (Fig. 1).

Low-Resolution Satellite Data. High-resolution ground truth data are extremely valuable but difficult to collect. Remote sensing offers a convenient alternative, with the drawbacks of a lower resolution and elaborate postprocessing and calibration.

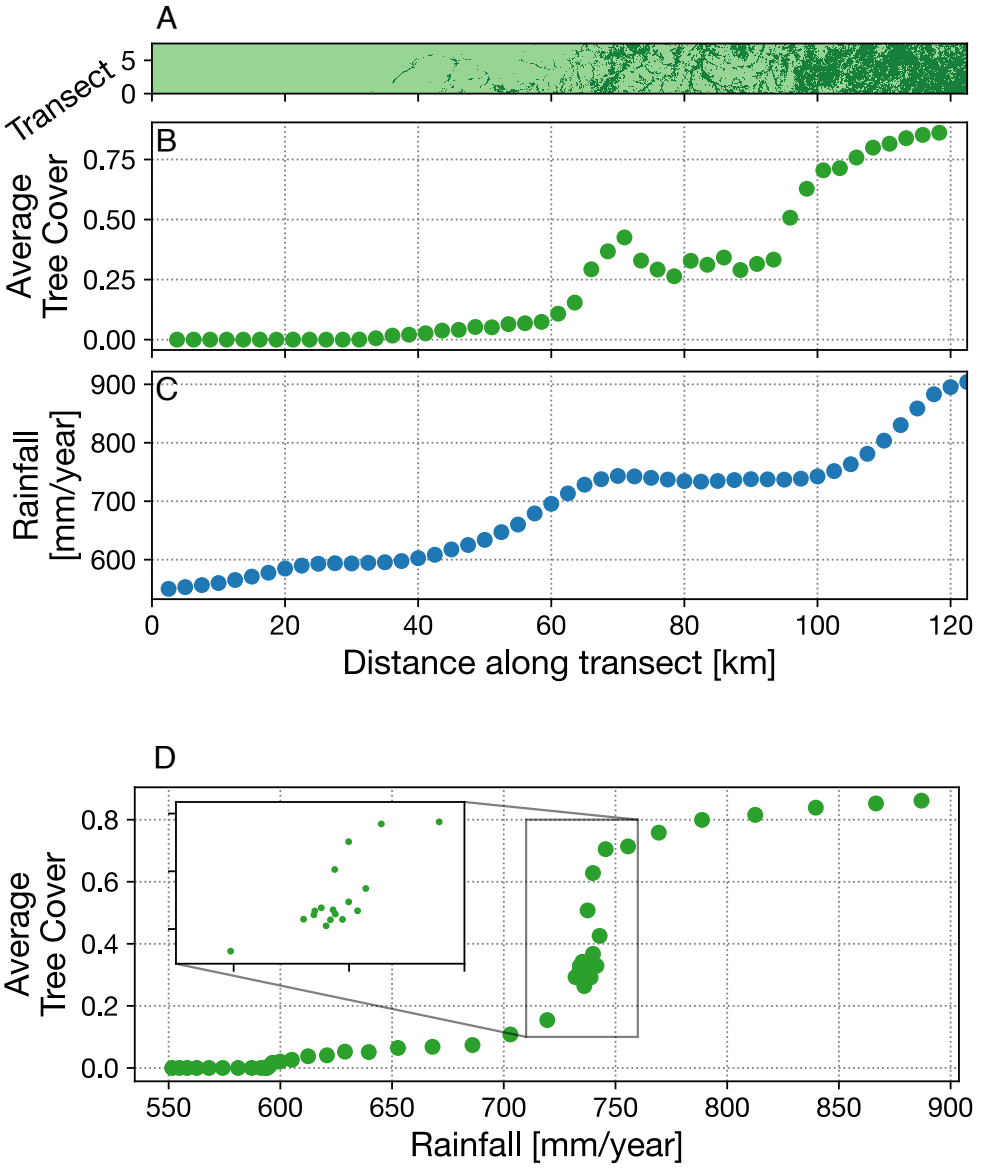

Fig. 1. (*A*) Serengeti–Mara Transect 5. Dark green represents woodland, while light green stands for grassland. (*B*) Average tree cover computed using a sliding 7.53-km-wide window and a 2.49-km step. (*C*) Mean annual rainfall along the transect. (*D*) Average tree coverage vs. mean annual rainfall. In the inset, a small hysteresis cycle is visible in the transition region.

For this study, we use satellite tree cover data from the Moderate Resolution Imaging Spectroradiometer (MODIS) at 250-m resolution (MOD44B) (24). Contrarily to the high-resolution dataset, here, each pixel represents a continuous variable: the proportion of tree coverage in a 250-m × 250-m patch. The transects have 200 × 4, 800 pixels; pixels occupied by rivers or water bodies have been disregarded in the calculations.

We combined the vegetation data with data from the Tropical Rainfall Measuring Mission (TRMM). Specifically, we used TRMM 3B43 mean annual rainfall data at 0.25-degree resolution (25), which we linearly interpolated at the vegetation grid level

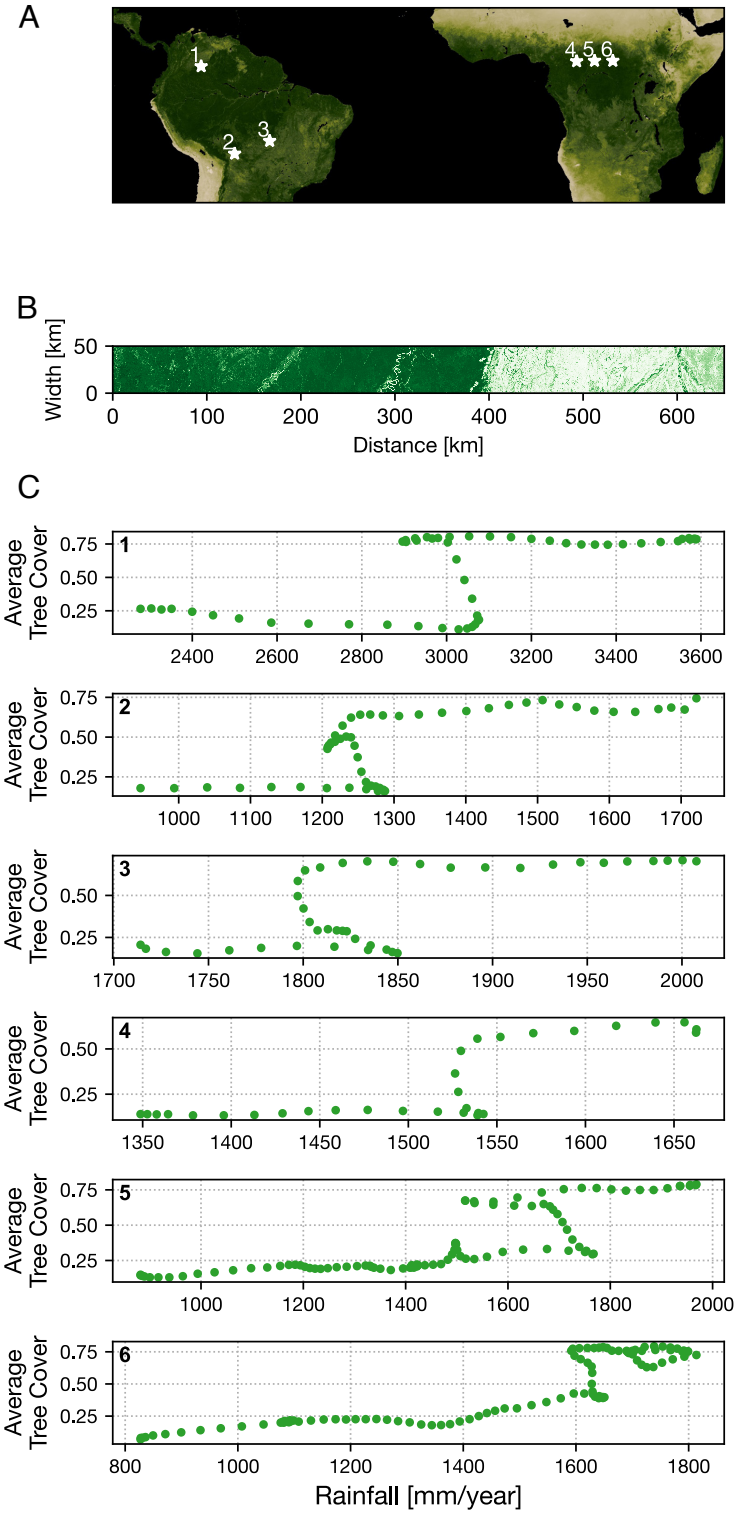

Fig. 2. (*A*) Locations of the six satellite-derived transects analyzed in this study. (*B*) Transect 1 tree cover as shades of green. (*C*) Average tree cover dependency on rainfall for the six transects. Abrupt transitions are visible for different rainfall thresholds.

to assign, to each vegetation pixel, a value of mean annual precipitation.

Regions of tree cover bistability in this dataset have been known for a long time, and they have been characterized and analyzed in several works (see e.g., refs. 26–28). We focus on regions of tropical forest–grassland transitions and analyze six transects in Central Africa and South America that show bistability and a relatively abrupt transition from one branch to the other (Fig. 2).

Models. Vegetation models are usually of the type of reaction–diffusion models or cellular automata (29, 30). Given that the empirical data we are considering is formed either by continuous or discrete pixel values, we studied one model of each category. Specifically, we simulated the local positive feedback (LPF) model describing the interaction between biomass and soil water in a 2D region (15, 31) and the local facilitation cellular automata (LFCA) model (32). The models' equations and parameters employed are presented in *SI Appendix*.

In the LPF model, a reaction–diffusion system presents bistability between an arid state (almost null biomass) and a vegetated branch. A transcritical bifurcation and a saddle-node delimitate the region of coexistence, the latter causing an abrupt collapse from the vegetated branch to the arid state as the rainfall decreases under a certain threshold.

The LFCA model, instead, describes the evolution of vegetation patches as a function of a wetness parameter, denoted as b in ref. 32. Each patch can either be occupied by trees or bare soil, and the probability of tree occupancy depends on different parameters, among which there is the mean state of the neighboring cells, which provides a form of local interaction. The model predicts a progressive degradation of the patches as the wetness parameter decreases, up to the point in which vegetation cannot self-sustain, and an abrupt transition to the arid state occurs (5).

Methodology

PE is a popular complexity measure for time series analysis (21, 22), as it is very simple to implement and robust to noise. It has also been adapted to the analysis of 2D images by defining 2D ordinal patterns (2D-OPs) (33), a technique that is useful to characterize the complexity of simulated cardiac arrhythmia data (34) as well as statistical properties of textures in images (35).

Formally, spatial PE is defined as the normalized Shannon entropy:

$$H = -\frac{1}{\log M}\sum_{i}^{M} p_i \log p_i, \qquad [1]$$

where p_i are the probabilities of the 2D-OPs, and M is the number of possible 2D-OPs. In the case of a continuous field, if the 2D-OPs are calculated with rectangles of X × Y pixels, then we have $M = (XY)!$ In the case of binary fields, instead, we have $M = 2^{XY}$. To examine properties at different spatial scales, one can use a lag and, in this case, the 2D-OPs are formed by nonneighboring data points (*SI Appendix* for further details).

The results presented in this study have been obtained using 2D-OPs formed with 2 × 2 neighboring data points. The effects of a lag and different choices for X and Y are discussed in *SI Appendix*.

As a reference, we compare the variation of the spatial PE with that of the spatial correlation. For a bidimensional spatial field u_{ij}, we calculated the spatial correlation as Moran's I coefficient (36):

$$I = \frac{N}{\sum_i \sum_j w_{ij}} \frac{\sum_i \sum_j w_{ij}(u_i - \bar{u})(u_j - \bar{u})}{\sum_i (u_i - \bar{u})^2}, \qquad [2]$$

where the coefficients w_{ij} are 1 if the points i and j are first neighbors and 0 otherwise, $\bar{u}$ is the average value of u_{ij}, and N is the total number of points.

Results

Fig. 3 displays the results of the analysis of the high-resolution vegetation data. It can be seen that the transition from the lower to the upper vegetation branch is characterized by a monotonous rise of the spatial PE (empty red symbols). The desertification transition (from the upper vegetation branch to the lower arid branch, filled red symbols) is also characterized by the increase of the spatial PE, although the increase is not as pronounced as in the transition from the lower to the upper branch.

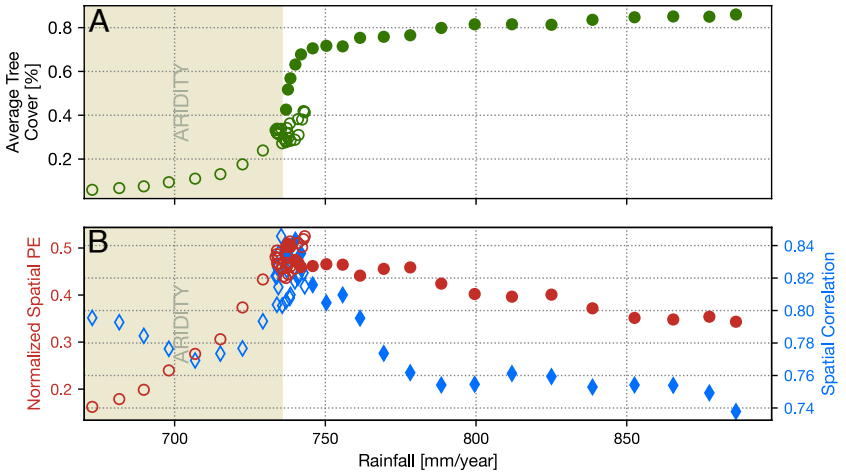

Fig. 3. Analysis of high-resolution vegetation data. (*A*) Average tree cover as a function of the mean annual rainfall; solid and empty symbols are used to differentiate the *Upper* and *Lower* branches. (*B*) Spatial permutation entropy (Eq. **1**, red) and spatial correlation (Eq. **2**, blue) of the tree cover field as a function of the mean annual rainfall. These quantities have been computed using a 7.5-km-wide window and a 1.23-km step.

Moran's I coefficient (shown with blue symbols) also provides a good early warning indicator of the transitions as in both branches, it rises when approaching the transition, as was already reported in ref. 20. In contrast to the spatial PE, the variation of the spatial correlation is more pronounced in the upper branch than in the lower one.

Therefore, the spatial PE and the spatial correlation provide complementary early indications of the approaching transition, as they both grow when the system moves toward the vegetation cover tipping point.

Fig. 4 displays the results of the analysis of transect 1 of the low-resolution vegetation data (the results obtained from the other transects are presented in *SI Appendix*). The average tree cover shows two clearly different states that overlap in a bistability region, where the rainfall ranges from 2,900 to 3,100 mm/y. Starting in the upper branch, when the mean annual rainfall decreases, both entropy and spatial correlation decrease, with the entropy rising back right before the transition. The rise of the entropy before the transition seems to be a robust indicator of the approaching tipping point as it occurs in the six transects studied. In contrast, the increase in spatial correlation before the transition is observed in 4 of 6 transects. (No increase is observed in transects 1 and 5.)

Interestingly, whenever the entropy reaches a minimum before the transition, this minimum is located at or near the beginning of the bistability region. We observe this in five of the six transects analyzed, with the exception of transect 2, in which no minimum is observed.

In the transition from the low to the high branch (i.e., from the arid to the vegetated state), the behavior of the two indicators is inconsistent across the different transects. In particular, the spatial PE is almost constant in transects 1, 5, and 6; grows in transects 2 and 3; and decreases in transect 4, while the spatial correlation increases in transect 6; decreases in transects 2, 3, and 4; and remains constant in transects 1 and 6.

Figs. 5 and 6 display the results obtained from the simulated data, with the LPF model and the LFCA model, respectively. In both cases, the entropy decreases before the transition to the desert state, while the spatial correlation increases. The only notable difference between the results obtained with the two models is seen in the behavior of the entropy far from the transition. In the case of the cellular automata, the entropy decreases with increasing wetness. Indeed, if the wetness is high enough, the simulated area will be filled with vegetated patches. Once the trees occupy the whole space, the entropy is zero. Hence, for high-enough wetness (far from the transition) the entropy is anticorrelated with the average tree cover, with a peak at 50% average tree cover. On the other side of the transition, if the wetness is low enough, the average tree cover tends to zero, as also the entropy.

Discussion

We have found, both in real and simulated vegetation data, that the behavior of the spatial permutation entropy as a function of the stress parameter is quite diverse. Taken together, our results show that the entropy changes when approaching a bifurcation, but the variation depends on the particular system under analysis.

In the simulated data, the variation of the entropy can be understood in terms of processes whose influence on the fields' spatial structure is known. In the LPF model, the spatial structure is determined by only two processes: the uncorrelated noise, which will produce a high spatial entropy, and the diffusion, which induces a first-neighbors coupling that reduces the entropy. In relative terms, the coupling will be strong when the system is close to the transition point. In Fig. 5*B*, we indeed observe this effect: as the rainfall parameter decreases, the entropy diminishes, even though its variation is small in absolute terms. This suggests that the entropy may be able to detect the increasing importance of spatial coupling, in spite of the fact that the field dynamics remain dominated by noisy fluctuations. This is consistent with the variation of the spatial correlation: as reported in refs. 15, 16, 23, 37, and 38, the spatial correlation increases as the transition approaches and constitutes the classic spatial indicator of critical slowing down. However, at least for the simulated data analyzed here, the variation of both indicators is rather modest.

In the LFCA model, similar findings can be interpreted as follows: as the state of each cell is either 1 (occupied by a tree) or 0 (unoccupied), the fully vegetated state and the desert state will both have zero entropy, as only one spatial ordinal pattern will be present.Therefore, before the transition, the entropy will likely go through one or more maximum values, as in Fig. 6*B*.

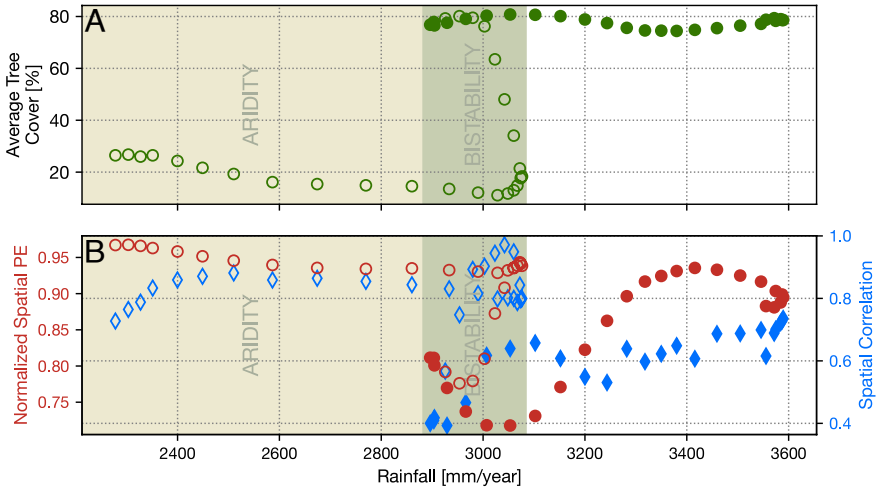

Fig. 4. Analysis of satellite vegetation data (transect 1). (*A*) Average tree cover as a function of the mean annual rainfall; solid and empty symbols are used to differentiate the *Upper* and *Lower* branches. (*B*) Spatial entropy (red) and spatial correlation (blue) of the tree cover field. These quantities have been computed using a 50-km-wide window and a 12.5-km step.

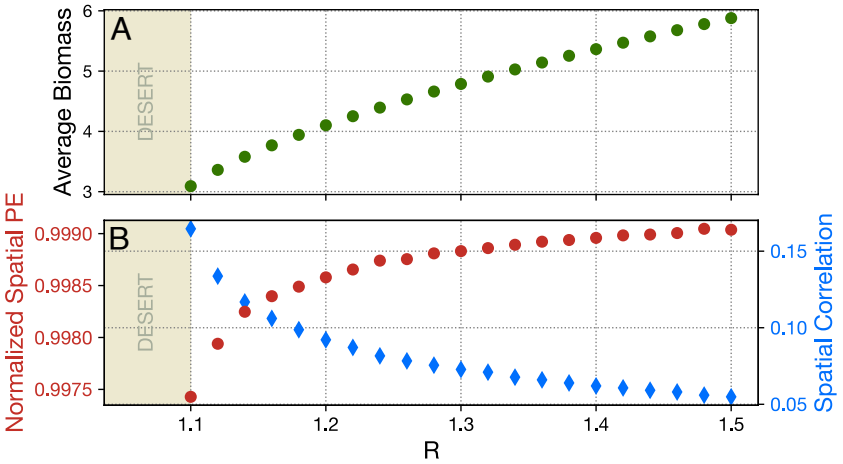

Fig. 5. Analysis of vegetation data simulated with the LPF model. (*A*) Average biomass as a function of the rainfall parameter, *R*. (*B*) Spatial PE (red) and spatial correlation (blue).

The moment when the entropy starts decreasing can be used as a precursor of the upcoming transition. A nonmonotonic indicator like the spatial PE has pros and cons when compared to an indicator as the spatial correlation, that varies monotonically when approaching the transition: on the one hand, the inflection point provides information of the closeness to the tipping point, but on the other hand, the existence of more than one extreme point will lead to false alarms. In contrast, an indicator that varies monotonically when approaching the transition does not provide any false alarm, but it does not provide information regarding the closeness to the tipping point.

For the two models and for the transects, we estimated the power of the spatial PE and of the spatial correlation following (39) and found that the spatial PE outperforms the spatial correlation for the LFCA model and the vegetation transects, while it underperforms for the LPF model (the comparison is presented in *SI Appendix*).

In the real data, the behavior of the spatial entropy and the spatial correlation differs from that found in simulated data and is harder to interpret. In the case of the high-resolution vegetation transect, as we see in Fig. 3, both the entropy and the spatial correlation increase when approaching the transition, and this occurs in both transition directions. This is in contrast with the LFCA model, which was proposed to explain the binary distribution of tree/grassland patches (32). Also, the values of entropy and spatial correlation are quite different in the real data and in the LFCA model simulations. In particular, the real data have lower entropy and higher correlation, indicating a higher spatial coherence. We speculate that this might be because the LFCA model, despite explaining relevant properties of the data—such as the rising spatial correlation approaching the transition from vegetated to arid state—does not fully reproduce the statistical spatial structure of the real tree cover distribution.

In the satellite transect data, the behavior of the entropy and the spatial correlation is different from those found in the high-resolution transect data. When moving toward the transition along the vegetated branch, the entropy decreases, and the spatial correlation also decreases monotonically, albeit irregularly (Fig. 4), which is opposite to the behavior expected before a tipping point.

We remark that tree cover is determined not only by the average rainfall but also by a multiplicity of other factors, such as soil type, altitude, and terrain slope, among others. If the decrease of the tree cover is governed by the variation of a different, unobserved parameter, it is possible that reordering the indicators

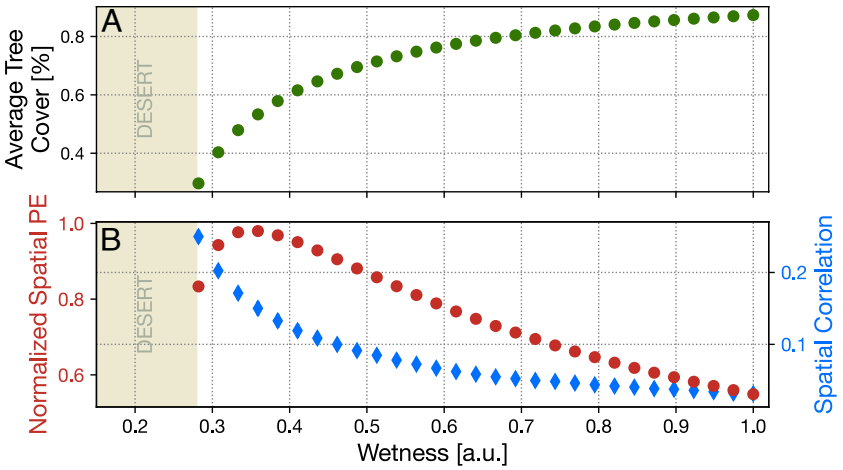

Fig. 6. Analysis of vegetation data simulated with the LFCA model. (*A*) Average tree cover as a function of the wetness parameter. The vegetation collapses into a desert state under a critical wetness level. (*B*) Spatial PE and spatial correlation.

according to this hidden variable will show the expected trend, i.e., the rise of spatial correlation.

We note that in all the low-resolution transects analyzed, the spatial entropy displays a smoother behavior than the spatial correlation, which is convenient because a smoother behavior can be expected to be less prone to false alarms once an early warning criterion is established.

Another interesting feature of the spatial entropy trend seen in the low-resolution vegetation data is that in the transition from the vegetated to the arid state, the minimum seems to coincide with the start of the bistability region, and this occurs in the five transects where there the entropy reaches a minimum value before the transition. This is a remarkable feature because it suggests that the spatial entropy detects a global change in the system's phase space (the appearance of a different state). However, further studies are needed to understand the physical mechanisms underlying this feature.

We are currently working to develop a model of tree cover bistability to more accurately reproduce the transect data we have analyzed to investigate the physical mechanisms that originate the minimum of the entropy. For example, some fire feedback models can produce flat savanna/forest branches separate by an abrupt transition (40), which seem well suited to reproduce phase diagrams as Fig. 4*A*.

Ecosystems can be expected to exhibit quite different spatial organizations when examined at different scales. In the high-resolution dataset, spanning roughly 100 km, we found that the system entropy is rather small, rising only in the transition zone. On the contrary, in the six low-resolution transects analyzed, the entropy of the arid branch is high, almost 1, while in the high-resolution data it is lower. Taken together, our results suggest that vegetated areas have, at a small spatial scale, a spatially organized tree cover (Fig. 3), which becomes more irregular at a large scale (Fig. 4), especially in regions of scarce tree cover.

Another possible explanation could be due to the fact that the spatial coupling of the patches of vegetation is too small at the 250-m × 250-m length-scale, to overcome the effect of noise. This is consistent with the observation that spatially coupled dynamical systems present bistability and hysteresis only if the spatial coupling is small enough (27).

Modeling tree cover bistability as a pair of saddle-nodes bifurcations has been shown useful for extracting information, from satellite tree cover data, about the forest/savanna coexistence (26). However, our results suggest that additional mechanisms are needed to fully understand the transition between the two states.

Conclusion

Using observational vegetation data and simulated data from two dynamical models, we have shown that the permutation entropy computed from the probabilities of spatial ordinal patterns can be a useful indicator of a forthcoming tipping point, complementing the information provided by a classical indicator such as the spatial correlation.

For the satellite transects, the permutation entropy has the advantage that it displays smaller relative fluctuations than the spatial correlation. Another interesting feature found is that, in the transition from the vegetated to the arid state, the minimum of the spatial permutation entropy seems to coincide with the start of the bistability region. Further studies are needed to understand the origin of this behavior.

We believe that the spatial PE can be able to provide an early warning indicator for other systems displaying CSD, and it will be interesting to test its potential in real-world systems aside from spatial vegetation fields. Both these directions of research are currently being pursued.

It is important to note that, as other indicators, the spatial PE has limitations: its variation can depend on the system and the data under study, and it is necessary to establish adequate criteria for detecting significant variations, which in turn could depend on the characteristics of the data, such as temporal or spatial resolution. Hence, we do not propose replacing existing spatial indicators with spatial PE but rather using spatial PE in conjunction with existing indicators or model-based approaches.

Our results suggest that the spatial PE can be a good indicator of an abrupt shift in vegetation, and we believe that it has promising applications in the remote monitoring of ecosystems.

Data, Materials, and Software Availability. The code used for the analysis is freely available via GitHub at https://github.com/giuliotirabassiupc/SPEV. Previously published data were used for this work (20, 25).

ACKNOWLEDGMENTS. We acknowledge the support of the ICREA ACADEMIA program of Generalitat de Catalunya and Ministerio de Ciencia e Innovación, Spain, project PID2021-123994NB-C21.

1. A. Hastings, D. B. Wysham, Regime shifts in ecological systems can occur with no warning. *Ecology Lett.* **13**, 464 (2010).
2. J. J. Jiang *et al*., Predicting tipping points in mutualistic networks through dimension reduction. *Proc. Natl. Acad. Sci. U.S.A.* **115**, E639–E647 (2018).
3. E. Hernandez-Garcia, C. Lopez, Sustained plankton blooms under open chaotic flows. *Ecol. Complexity* **1**, 253 (2004).
4. D. Ortiz, J. Palmer, G. Wilkinson, Detecting changes in statistical indicators of resilience prior to algal blooms in shallow eutrophic lakes. *Ecosphere* **11**, e03200 (2020).
5. S. Kefi *et al*., Spatial vegetation patterns and imminent desertification in mediterranean arid ecosystems. *Nature* **449**, 213 (2007).
6. A. F. Almeida-Naunay *et al*., Recurrence plots for quantifying the vegetation indices dynamics in a semi-arid grassland. *Geoderma* **406**, 115488 (2022).
7. T. M. Lenton *et al*., Tipping elements in the earth's climate system. *Proc. Natl. Acad. Sci. U.S.A.* **105**, 1786 (2008).
8. M. Scheffer *et al*., Anticipating critical transitions. *Science* **338**, 344 (2012).
9. S. R. Carpenter, W. A. Brock, Rising variance: A leading indicator of ecological transition. *Ecol. Lett.* **9**, 308–315 (2006).
10. V. Dakos *et al*., Robustness of variance and autocorrelation as indicators of critical slowing down. *Ecology* **93**, 264–271 (2012).
11. V. Dakos *et al*., Slowing down as an early warning signal for abrupt climate change. *Proc. Natl. Acad. Sci. U.S.A.* **105**, 14308 (2008).
12. N. Boers, M. Rypdal, Critical slowing down suggests that the western greenland ice sheet is close to a tipping point. *Proc. Natl. Acad. Sci. U.S.A.* **118**, e2013349118 (2021).
13. M. Marconi *et al*., Testing critical slowing down as a bifurcation indicator in a low-dissipation dynamical system. *Phys. Rev. Lett.* **125**, 134102 (2020).
14. C. D. Buelo *et al*., Evaluating the performance of temporal and spatial early warning statistics of algal blooms. *Ecol. Appl.* **32**, 2626 (2022).
15. V. Guttal, C. Jayaprakash, Spatial variance and spatial skewness: Leading indicators of regime shifts in spatial ecological systems. *Theor. Ecol.* **2**, 3–12 (2009).
16. V. Dakos, E. H. van Nes, R. Donangelo, H. Fort, M. Scheffer, Spatial correlation as leading indicator of catastrophic shifts. *Theor. Ecol.* **3**, 163–174 (2010).
17. S. R. Carpenter, W. A. Brock, Early warnings of regime shifts in spatial dynamics using the discrete Fourier transform. *Ecosphere* **1**, 1–15 (2010).
18. V. Dakos, S. Kéfi, M. Rietkerk, E. H. Van Nes, M. Scheffer, Slowing down in spatially patterned ecosystems at the brink of collapse. *Am. Nat.* **177**, E153–E166 (2011).
19. G. Oborny, B. György Szabó, Dynamics of populations on the verge of extinction. *Oikos* **109**, 291–296 (2005).
20. S. Eby, A. Agrawal, S. Majumder, A. P. Dobson, V. Guttal. Alternative stable states and spatial indicators of critical slowing down along a spatial gradient in a savanna ecosystem. *Global Ecol. Biogeogr.* **26**, 638–649 (2017). 10.1111/geb.12570.
21. C. Bandt, B. Pompe, Permutation entropy: A natural complexity measure for time series. *Phys. Rev. Lett.* **88**, 174102 (2002).
22. I. Leyva, J. H. Martinez, C. Masoller, O. A. Rosso, M. Zanin, 20 years of ordinal patterns: Perspectives and challenges. *EPL* **138**, 31001 (2022).
23. D. N. Reed, T. Michael Anderson, J. Dempewolf, K. Metzger, S. Serneels, The spatial distribution of vegetation types in the Serengeti ecosystem: The influence of rainfall and topographic relief on vegetation patch characteristics. *Biogeogr. J.* **36**, 770–782 (2009).
24. C. Dimiceli, M. Carroll, R. Sohlberg, D. H. Kim, M. Kelly, J. Townshend, MOD44B MODIS/Terra vegetation continuous fields yearly L3 global 250m SIN grid V006 [data set]. NASA EOSDIS land processes DAAC (2015). 10.5067/MODIS/MOD44B.006. Accessed 24 March 2021.
25. Tropical Rainfall Measuring Mission (TRMM), TRMM (TMPA/3B43) Rainfall Estimate L3 1 month 0.25 degree x 0.25 degree V7, Greenbelt, MD, Goddard Earth Sciences Data and Information Services Center (GES DISC, 2011). https://disc.gsfc.nasa.gov/datasets/TRMM_3B43_7/summary. Accessed 25 July 2022.

26. C. Ciemer *et al*., Higher resilience to climatic disturbances in tropical vegetation exposed to more variable rainfall. *Nat. Geosci.* **12**, 174–179 (2019). 10.1038/s41561-019-0312-z.
27. A. Staal, S. C. Dekker, C. Xu, E. H. van Nes, Bistability, spatial interaction, and the distribution of tropical forests and savannas. *Ecosystem* **19**, 1080–1091 (2016).
28. B. Wuyts, A. R. Champneys, J. I. House, Amazonian forest-savanna bistability and human impact. *Nat. Commun.* **8**, 1–12 (2017).
29. F. Borgogno, P. D'Odorico, L. Laio, L. Ridolfi, Mathematical models of vegetation pattern formation in ecohydrology. *Rev. Geophys.* **47**, RG1005 (2009).
30. H. Balzter, P. W. Braun, W. Köhler, Cellular automata models for vegetation dynamics. *Ecol. Modell.* **107**, 113–125 (1998).
31. G. Tirabassi *et al*., Interaction network based early-warning indicators of vegetation transitions. *Ecol. Complexity* **19**, 148–157 (2014).
32. S. Kéfi, M. Rietkerk, M. van Baalen, M. Loreau, Local facilitation, bistability and transitions in arid ecosystems. *Theor. Popul. Biol.* **71**, 367–379 (2007).
33. H. V. Ribeiro, L. Zunino, E. K. Lenzi, P. A. Santoro, R. S. Mendes, Complexity-entropy causality plane as a complexity measure for two-dimensional patterns. *PLoS One* **7**, e40689 (2012).
34. A. Schlemmer *et al*., Spatiotemporal permutation entropy as a measure for complexity of cardiac arrhythmia. *Front. Phys.* **6**, 39 (2018).
35. H. Y. D. Sigaki, R. F. de Souza, R. T. de Souza, R. S. Zola, H. V. Ribeiro, Complexity-entropy causality plane as a complexity measure for two-dimensional patterns. *Phys. Rev. E* **99**, 013311 (2019).
36. P. A. P. Moran, Notes on continuous stochastic phenomena. *Biometrika* **37**, 17–23 (1950).
37. V. Dakos, E. H. Van Nes, P. d'Odorico, M. Scheffer, Robustness of variance and autocorrelation as indicators of critical slowing down. *Ecology* **93**, 264–271 (2012).
38. J. Van Belzen *et al*., Vegetation recovery in tidal marshes reveals critical slowing down under increased inundation. *Nat. Commun.* **8**, 1–7 (2017).
39. C. Boettiger, A. Hastings, Quantifying limits to detection of early warning for critical transitions. *J. R. Soc. Int.* **9**, 2527–2539 (2012).
40. A. Staal, S. C. Dekker, M. Hirota, E. H. van Nes, Synergistic effects of drought and deforestation on the resilience of the south-eastern Amazon rainforest. *Ecol. Complexity* **22**, 65–75 (2015).